First publ. in: Journal of Geophysical Research 102 (1997), No. C13, pp. 27,903-27,914

Boundary versus internal diapycnal mixing in stratified natural waters

G.-H. Goudsmit, F. Peeters, M. Gloor,[1] and A. Wüest

Department of Environmental Physics, Swiss Federal Institute of Environmental Science and Technology (EAWAG) and Swiss Federal Institute of Technology (ETH), Dübendorf

Abstract. Using the fluorescent dye uranin, tracer release experiments to study the contribution of bottom boundary mixing to diapycnal transport in stratified natural waters were performed in Lake Alpnach (central Switzerland) during 1992-1995. A first experiment involved injecting the tracer from a point source into the center of the hypolimnion (that part of the lake below the surface mixed layer). An in situ fluorometer was then employed to detect the horizontal and vertical spreading of the tracer cloud, allowing rates of diapycnal diffusivity to be determined. As long as the tracer was confined to the interior water region, the diapycnal diffusivity was relatively small. However, after the tracer cloud had reached the lake boundary, the diapycnal diffusivity increased by approximately one order of magnitude. In a second experiment, the tracer was released near the sediment-water interface. In this case the dynamics of vertical tracer spreading were opposite. During the first few hours after tracer release, diapycnal diffusivities were large, subsequently decreasing as the tracer cloud drifted away from the lake boundary. Basin-wide diapycnal diffusivities calculated from heat flux measurements based on temperature profiles obtained from thermistor chains or conductivity-temperature-depth casts agreed well with the values obtained from the vertical tracer diffusion after horizontal homogenization. The results of the tracer experiments corroborate the hypothesis that diapycnal fluxes are determined predominantly by mixing in the bottom boundary region.

1. Introduction

Diapycnal mixing, i.e., mixing across surfaces of equal density, is one of the most important physical process in lakes and oceans. It controls the vertical distribution of biological and chemical constituents, for instance, and is thus of major ecological relevance.

Diapycnal mixing in stratified natural water bodies has been studied using various techniques, e.g., temperature microstructure or shear measurements, tracer spread experiments, and budgeting (natural) tracers. A survey of various methods and studies has been given by *Gregg* [1987].

Estimates of the diapycnal diffusivity in the thermocline of lakes and oceans using microstructure techniques [e.g., *Gregg*, 1987; *Toole et al.*, 1994; *Wüest et al.*, 1996] differ by about one order of magnitude from those based on basin-wide tracer balances [e.g., *Munk*, 1966; *Gargett*, 1984]. A possible explanation for this discrepancy is the presence of enhanced mixing at the bottom boundary of the basin and its effect on the mean effective diapycnal transport. *Munk* [1966] and *Armi* [1978] suggested that diapycnal mixing in the bulk water might be small compared to mixing at the bottom boundaries and that the overall diapycnal transport should therefore be considered as a composition of the two processes.

[1]Now at Atmospheric and Oceanic Science Program, Princeton University, Princeton, New Jersey.

A common explanation for enhanced bottom boundary mixing is the current-induced shear instability at the sediment [*Thorpe*, 1988]. An alternative mechanism leading to enhanced mixing at basin boundaries is the reflection of internal waves impinging on sloping bottom boundaries at critical angles [*Eriksen*, 1982; *Garrett*, 1991]. Enhanced mixing at bottom boundaries leads to well-mixed layers with respect to temperature and salinity near the sediment-water interface. Such layers (so-called benthic boundary layers) have been found in oceans [e.g., *Armi*, 1978; *Ivey*, 1987; and references therein] and lakes [*Gloor et al.*, 1994]. *Gloor* [1995] demonstrated that the thickness of the boundary layer near the deepest part of a lake is correlated with the energy loss of the bottom currents. These observations are in agreement with results of several authors [e.g., *Lueck et al.*; 1983, *Wüest et al.*, 1996] who found a remarkable increase in energy dissipation within the boundary layer using microstructure techniques.

However, *Garrett* [1991] pointed out that intense turbulence within the boundary layer does not necessarily lead to an increase in diapycnal transport, since the water to be mixed has almost the same temperature and salinity, i.e., is already well-mixed. In addition, *Peeters* et al. [1997] suggested that the development of a nearly homogeneous boundary layer in lakes does not necessarily require an increase in diapycnal mixing within the boundary layer.

Despite the intense discussion on boundary mixing in the literature, experimental evidence for the role of boundary mixing in natural waters on the overall diapycnal transport is rare. Such evidence is based mainly on the discrepancy between the turbulent fluxes calculated from microstructure measurements and those calculated from budgets of basin-wide tracers. *McDougall* [1984, 1987] has demonstrated that this discrepancy might be

explainable without requiring increased boundary mixing. According to *McDougall* [1987] advection along neutral surfaces in combination with the thermobaric effect would lead to transport through the neutral surfaces. As vertical turbulence is not required for this process, it is not detectable using microstructure techniques. However, this process requires pressure gradients along neutral surfaces. This effect is therefore expected to be negligible in the case of small or medium-sized basins where neutral surfaces are horizontal in the interior water.

To investigate empirically the role of bottom boundary mixing, *Wüest et al.* [1996] conducted an experiment in a lake where microstructure measurements were carried out to distinguish between interior water and near-boundary regions. The mean energy dissipation calculated from these measurements was shown to provide a diapycnal diffusion coefficient which was in good agreement with the spread of an SF_6 tracer cloud and with the transport of heat. A further indication of the importance of boundary mixing is provided by a tracer experiment in the open ocean [*Ledwell et al.*, 1993]. In this work, the diapycnal diffusion coefficient calculated from the vertical spread of tracer clouds was small compared to typical basin-wide diffusivities. Recently, *Ledwell and Bratkovich* [1995] demonstrated that this low diffusivity found in the interior water increases rapidly when the tracer meets the basin bottom boundaries [*Ledwell and Hickey*, 1995].

In this contribution we follow the work of *Ledwell and Bratkovich* [1995] to investigate the role played by the basin boundaries for the overall vertical transport in the hypolimnion of a lake using an artificial tracer. The main goal of our investigation was to determine the relative contributions of mixing in the bulk water and mixing at the bottom boundary to the mean basin-wide diapycnal transport. To accomplish this, two types of tracer experiment were conducted.

In the first type, a tracer patch was released into the middle of the lake, close to a predefined isopycnal surface. The release was designed to keep the initial vertical variance as small as possible. In the first few days following the release, the tracer in the interior water is subject to weak vertical mixing and to strong horizontal mixing. If mixing close to the lake boundary causes fast diapycnal transport, the rate of vertical spreading of the tracer cloud should increase after the tracer has reached the boundary region. After some time the tracer will be distributed homogeneously across the horizontal isopycnal surface; the tracer cloud should then "feel" both boundary and interior water mixing.

In the second type of experiment the tracer was again injected close to a predefined isopycnal surface, but this time close to the sediment-water interface. In this case, boundary mixing should have an immediate effect on the vertical distribution of the tracer, and the diapycnal diffusion rates should be large in the early stages of the experiment (when most of the tracer is located in the boundary region), and decrease afterwards.

As both approaches lead to a chronological separation between interior water, basin-wide, and boundary mixing, the experimental results should allow the contribution of internal and boundary mixing to the mean diapycnal diffusion experienced by basin-wide tracers (e.g., heat) to be analyzed. The mixing rates obtained from the tracer experiments were therefore compared with the basin-wide diffusion coefficients computed from continuously measured temperature profiles using the heat budget method of *Powell and Jassby* [1974].

In the following paragraphs we first present the experimental setup. We then describe the method of data analysis and present and discuss the results. The major results of the work are summarized in the last section.

2. Experiments

2.1. Experimental Site

The experimental work was carried out in Lake Alpnach, the smallest (surface area 4.8 km^2) basin of Lake Lucerne, situated in central Switzerland. The lake is approximately elliptical, is relatively shallow (maximum depth of 34 m), and is separated from the main part of the lake by a shallow sill. Major river input (Sarner Aa) consists of warm epilimnetic water from another lake, which consequently merges into the epilimnion of Lake Alpnach. Two smaller streams enter the lake, but in the absence of thunderstorms their discharges can be neglected. The hypolimnion of Lake Alpnach is therefore decoupled both from inflowing river water and from the Lake Lucerne water masses. Consequently, in the absence of flood-induced density currents, wind is the main driving force for the generation of turbulence in the hypolimnion.

During the summer months, convection produced by solar heating along the mountain slopes stimulates a predominant diel wind that blows regularly and uniformly parallel to the major axis (Figure 1). Lake Alpnach often experiences first and second vertical mode seiches [*Münnich et al.*, 1992]. As a consequence of the currents due to these oscillations, the benthic boundary layer is relatively well mixed and its thickness varies, depending on the depth and the strength of the seiche oscillations, over a few meters [*Gloor et al.*, 1994].

2.2. Experimental Setup

As is known from previous tracer experiments in various lakes [e.g., *Peeters et al.*, 1996] the horizontal distribution of a tracer cloud can become very inhomogeneous after a few days. To prevent time-consuming sampling and subsequent laboratory analysis, necessary in the case with tracers such as SF_6 [*Ledwell and Watson*, 1991; *Schlatter et al.*, 1990], the tracer should be detectable in situ. Fluorescent dyes are most suitable for this, as they can be directly detected in the water column by an appropriate fluorometer. Fluorescent dyes have been regularly used for tracer dispersion studies in oceans [e.g., *Okubo*, 1971]. For experiments in lakes, uranin (sodium fluorescein) is an appropriate optical tracer [*Leibundgut*, 1982] as it not only shows high fluorescence efficiency and low adsorbance to particulate and organic matter, but is also nontoxic to aquatic organisms [*Smart*, 1982]. With our experimental setup, uranin concentrations were detectable in situ within a large dynamic range of approximately four orders of magnitude (0.01-700 mg m^{-3}). This setup was therefore well-suited to explore development of the tracer distribution during the entire experiment. Since our experiments were conducted in the hypolimnion of a eutrophic lake, tracer loss due to photolysis [*Behrens and Teichmann*, 1982] is negligible.

The concentration of uranin was measured at a high sampling rate (10 Hz) by an in situ fluorometer (Dr. Haardt, Klein-Barkau, Germany) attached to a commercial conductivity-temperature-depth (CTD) probe (Meerestechnik-Elektronik, Trappenkamp, Germany). This equipment allowed the simultaneous measurement of depth, temperature, salinity, transmissivity, and uranin concentration. The ship position was determined using a microwave positioning system (Del Norte

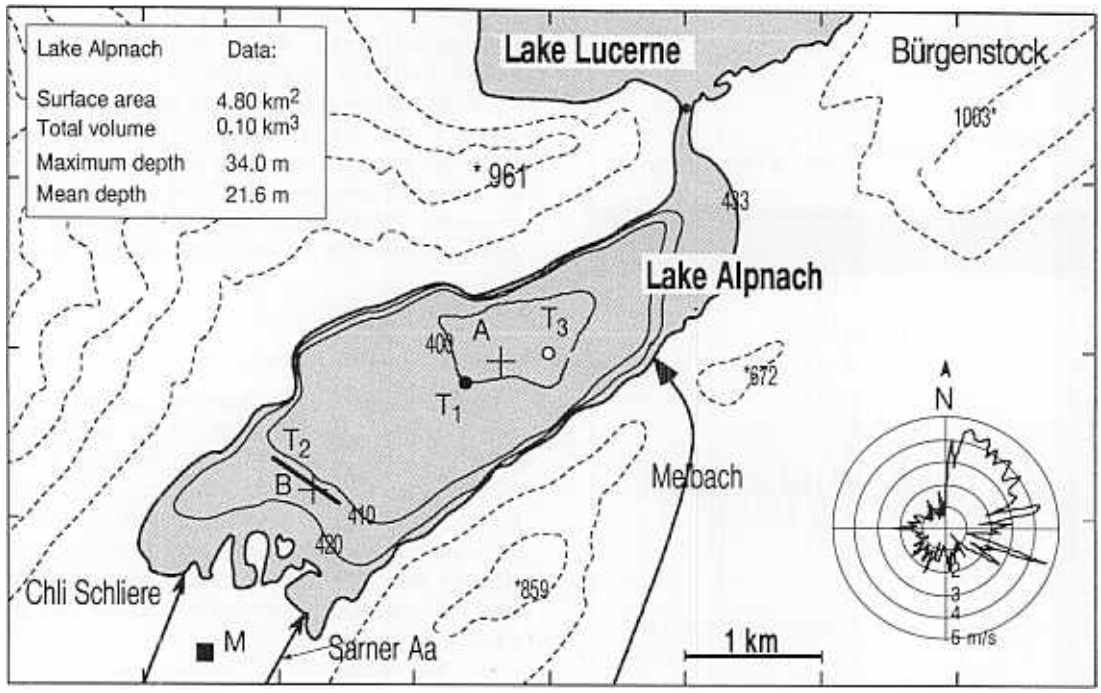

Figure 1. Map of Lake Alpnach (a side basin of Lake Lucerne, Switzerland). The positions (or region) of the tracer releases on October 12, 1992 (experiment I), June 13, 1994 (experiment II), and June 19, 1995 (experiment III), are labeled T_1 (solid circle), T_2 (heavy line) and T_3 (open circle), respectively. The locations of the thermistor strings moored in 1995 (A, 34 m; B, 22 m) are denoted by pluses. Depth contours, the lake surface elevation, and the heights of nearby mountains are given in meters above sea level. The inset gives the wind speed distribution measured in 1995 at the weather station M near the airport at Alpnach (solid square).

Technology Inc., Euless, Texas, U.S.A.) with a frequency of about 1 Hz and a horizontal resolution of approximately 1 m. All the instruments were connected to an automatic data acquisition system [*Peeters and Wüest*, 1992) that allowed on-line data display of the horizontal and vertical tracer distribution.

2.3. Tracer Injections

For this investigation, three experiments were conducted in 1992, 1994, and 1995. In the following, we will address these in chronological order as experiments I, II, and III, respectively. In all three experiments, uranin was first dissolved in (warm) surface water on board the measuring ship, pumped to the target depth, and released through eight nozzles, each with a diameter of 3.5 mm.

In October 1992, experiment I was conducted by injecting two solutions, each consisting of 500 g uranin dissolved in 50 L of surface water, into the middle of the lake at depths of 12 and 23 m. The goal was to inject the tracer as close as possible to a predefined isothermal surface within a small horizontal area. The location of the injection plume is shown in Figure 1. During the first few hours after the uranin release, no measurements were made because of the danger of causing serious distortions in the vertical tracer distributions in the initial, highly concentrated tracer clouds. Shortly after the release, the two tracer clouds drifted apart from each other, which complicated their detection, since in a given CTD yo-yo cast often only one of the tracer clouds was struck. Therefore no quantitative information on horizontal spreading could be obtained. This was one of the main reasons for repeating this tracer experiment in 1995 (experiment III).

Experiment III was started on June 19, 1995. A solution of 1.5 kg uranin in 110 L of surface water was released in the lower part of the hypolimnion at 25 m depth. Tracer concentrations at the end of experiment I had been rather low; consequently, because we planned to survey the tracer cloud over a duration of approximately 1 month in experiment III, the initial amount of uranin was increased. Additionally, a homemade drifter was installed prior to injection to allow the center of the tracer patch to be located quickly. For an exact daily survey of the tracer cloud, up to 500 profiles had to be recorded.

In contrast to experiments I and III, in which the tracer was injected approximately as a point-like source within a small horizontal area in the middle of the lake, in Experiment II (June 1994) the tracer was released along a line approximately 700 m in length (Figure 1) near the southwest shore, about 2 m above the sediment-water interface, close to the 7.42°C isothermal surface (i.e., isopycnal surface; density variations due to salinity gradients are negligible compared to temperature). Compared to experiments I and III, minimizing the initial vertical tracer distribution was more difficult because of the movement of the ship. Therefore a small CTD probe was mounted close to the nozzles of the injection tube to monitor the water temperature at which the tracer was injected and to control the vertical distance between injection tube and lake bottom. During tracer injection the nozzles were kept as close as possible to the depth corresponding to the predefined temperature, while deviations were adjusted by raising or lowering the injection tube. The recorded temperature profile and height above the sediment are plotted in Figure 2.

The amount of uranin released was reduced to 45 g, as the

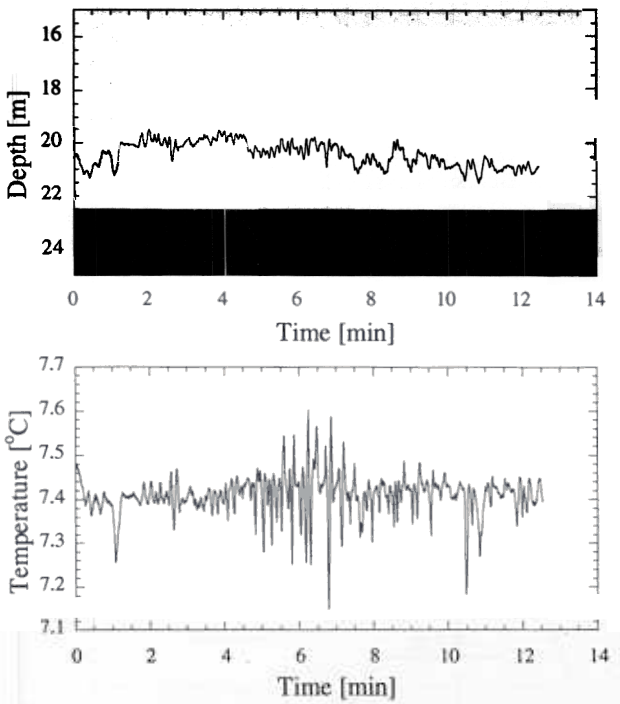

Figure 2. Tracer release on June 13, 1992 (experiment II) approximately 2 m above the sediment-water interface. Temperature and distance above sediment were measured by a small CTD probe mounted close to the nozzles of the injection tube.

total duration of the experiment was only a few days. It was expected that the effect of boundary mixing would occur immediately after the injection. Hence the initial tracer cloud was also surveyed intensively, and in contrast to experiments I and III, the number of measurements conducted immediately after the tracer release was increased. In experiment II the distortion of the tracer cloud by artificial mixing induced by the CTD casts was not critical because the initial area of the tracer cloud was much larger (Figure 1). Consequently, the total number of CTD casts could be raised without increasing the number of casts per unit lake area.

2.4. Thermistor Chains and Weather Station

In order to calculate the basin-wide diapycnal diffusivity by the heat budget method [*Powell and Jassby*, 1974] and to monitor the internal seiching, the lake water temperature was measured quasi-continuously by moored thermistor chains (Aanderaa, Bergen, Norway), consisting of 11 evenly-spaced sensors with a resolution of 0.023 K and a sampling rate of 0.2 min^{-1}. In June-July 1995 two thermistor chains were installed in series (from 1 to 11 m and 14 to 34 m) at position A (Figure 1), and another thermistor chain (1 to 21 m) was moored at position B. In June 1994, two thermistor chains (each 20 m long) were installed near positions A and B. In the prototype experiment in 1992, no thermistor chains were deployed. In this case, averaged CTD temperature profiles were used for the computation of basin-wide diapycnal diffusion coefficients.

Only in the last experiment in 1995 were meteorological quantities such as wind speed, air temperature, and solar radiation measured by a weather station (Aanderaa, Bergen, Norway). This weather station was installed at the airport near the lake (Figure 1) to rule out the possibility of a sudden spreading of the tracer patch being due to strong storm surges, and to compare the development of the spreading of the tracer with the meteorological forcing driving the mixing in the lake. All meteorological variables were measured every 10 min at a height of 5 m (not at the standard height of 10 m because of safety regulations in force at the airport). During the two other measuring campaigns, no weather stations were installed near the lake. However, qualitative information was still available from two nearby meteorological stations (at Lucerne and Mount Pilatus) maintained by the Swiss Meteorological Institute.

3. Data Analysis

3.1. Horizontal Distribution of the Tracer Cloud

The fluorometer was calibrated for uranin in the laboratory over the entire detection range of the instrument (0.01-700 mg m^{-3}). Natural fluorescence in the lake is rather small (corresponding to an uranin concentration of ~0.3 mg m^{-3}). However, to obtain genuine signals, this offset had to be carefully subtracted from the raw data set. This correction was particularly necessary about 1 month after tracer injection, as the genuine signal had decreased approximately to natural background levels by this time.

The first stage of the analysis involved exploring the horizontal spreading of the tracer patch. For each day separately, all concentration profiles (up to 500) were vertically integrated. The resulting horizontal mass distributions (mg m^{-2}) were interpolated horizontally using a kriging algorithm (Surfer, Golden Software Inc., Golden, U.S.A.) to obtain isoconcentration areas. An example of such an integration is given in Plate 1, which shows the isoconcentration areas for 1, 4, 7, 10, 18, and 28 days after the tracer injection of experiment III. For this type of experiment it is crucial to monitor carefully when the tracer reaches the bottom boundary at the depth of tracer release. Therefore in addition to the surface shore line, the line of the bottom boundary at the depth of the tracer cloud (25 m) is shown in Plate 1. The latter represents the real horizontal boundary for the tracer inside the lake basin.

Horizontal advection is responsible for the movement of the center of the tracer patch, while the spreading of the tracer relative to the center is due to diffusion. As can be seen from Plate 1, the tracer distributions are not radially symmetric but are rather inhomogeneous and exhibit more than one single maximum. This behavior has been observed in previous tracer experiments in Lake Alpnach [*Peeters et al.*, 1996]. During the first week after tracer release in experiment III, the cloud drifted in a counterclockwise direction toward the southwest shore of the lake, but without coming into contact with the bottom boundary. Subsequently, after about 1 week, the tracer cloud reached the western bottom boundary. Finally, at the end of the experiment after about 1 month, the tracer was nearly homogeneously spread over the entire lake area at tracer depth.

Due to the horizontal inhomogeneity of tracer clouds, much more information is needed to investigate the horizontal development of tracer clouds than is needed to investigate the vertical development. As was mentioned in section 2, fewer data were collected in experiment I than in experiment III, so that in experiment I there was not sufficient information to quantify the horizontal spreading of the tracer cloud accurately enough.

3.2. Mass Balance

A consistency check in tracer studies is to verify tracer mass conservation. For the first 2 weeks of experiment III, the total mass of the tracer was determined from the vertically integrated

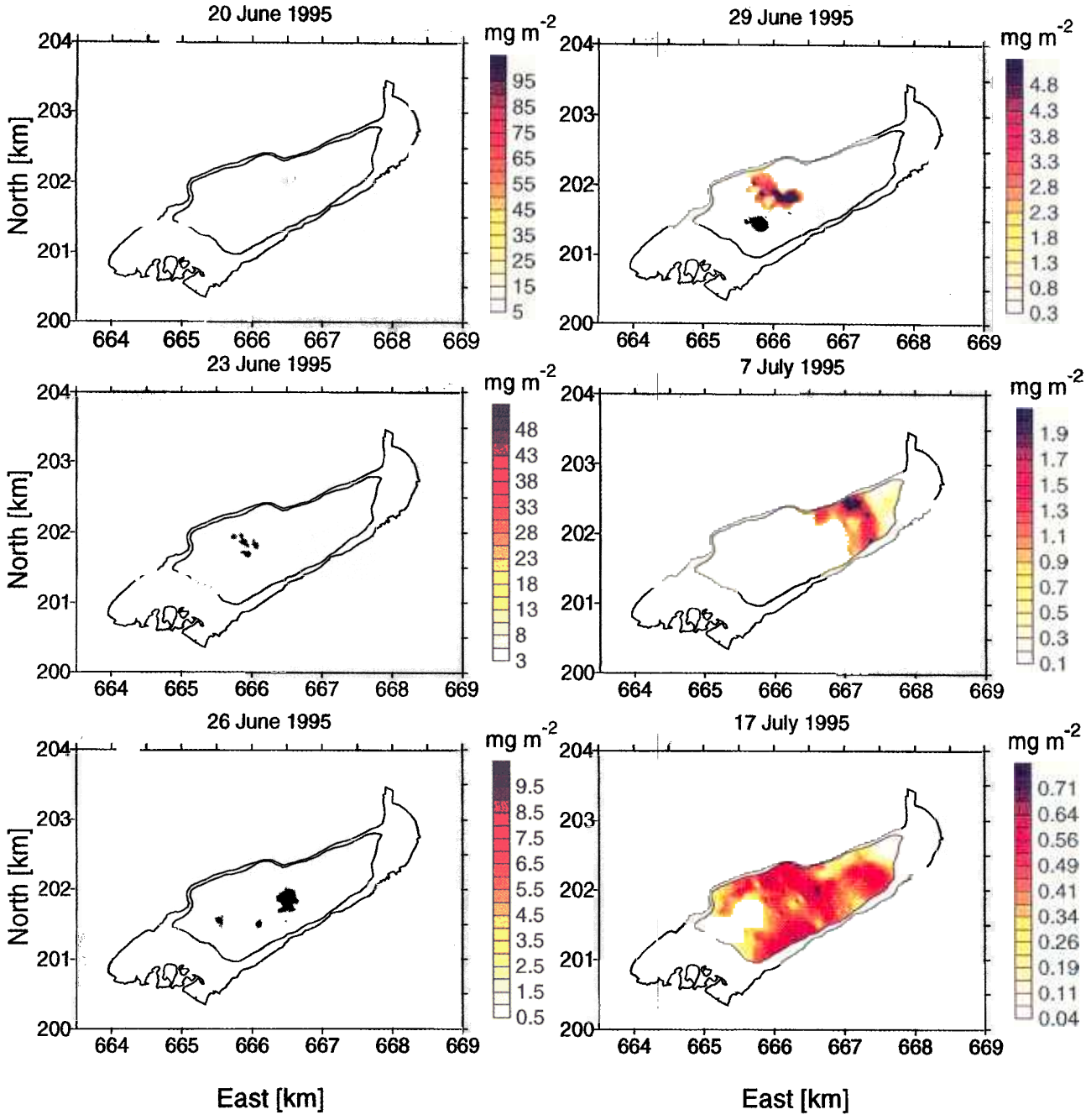

Plate 1. Horizontal distribution of uranin concentration after (left) 1, 4, and 7 days and (right panel) 10, 18, and 28 days after its point release on June 19, 1995 into the central hypolimnion of Lake Alpnach. The positions are given in terms of the Swiss Coordinate System.

and horizontally interpolated concentration profiles, as explained above.

During this period a total mass of (90±10)% of the initially released tracer was accounted for. This indicates that the photochemically induced depletion of uranin is rather small and that the determination of the extent of the tracer cloud in our experiments was excellent. After 2 weeks the tracer cloud was spread over almost the entire area of the lake at tracer depth. An accurate determination of the total tracer mass for that period of the experiment would have required a vast number of fluorometer casts.

3.3. Vertically Averaged Tracer Profiles

In order to obtain genuine mean vertical tracer profiles free from the distortions induced by internal seiching, the tracer concentration profiles from each day were averaged over horizontal areas of equal density, not of equal depth. This procedure enabled us to calculate a mean concentration versus density dependence, removing the effect of displacements of the water layers relative to the equilibrium depth. Finally, from the daily-averaged density profile, the mean profiles of concentration versus depth were calculated.

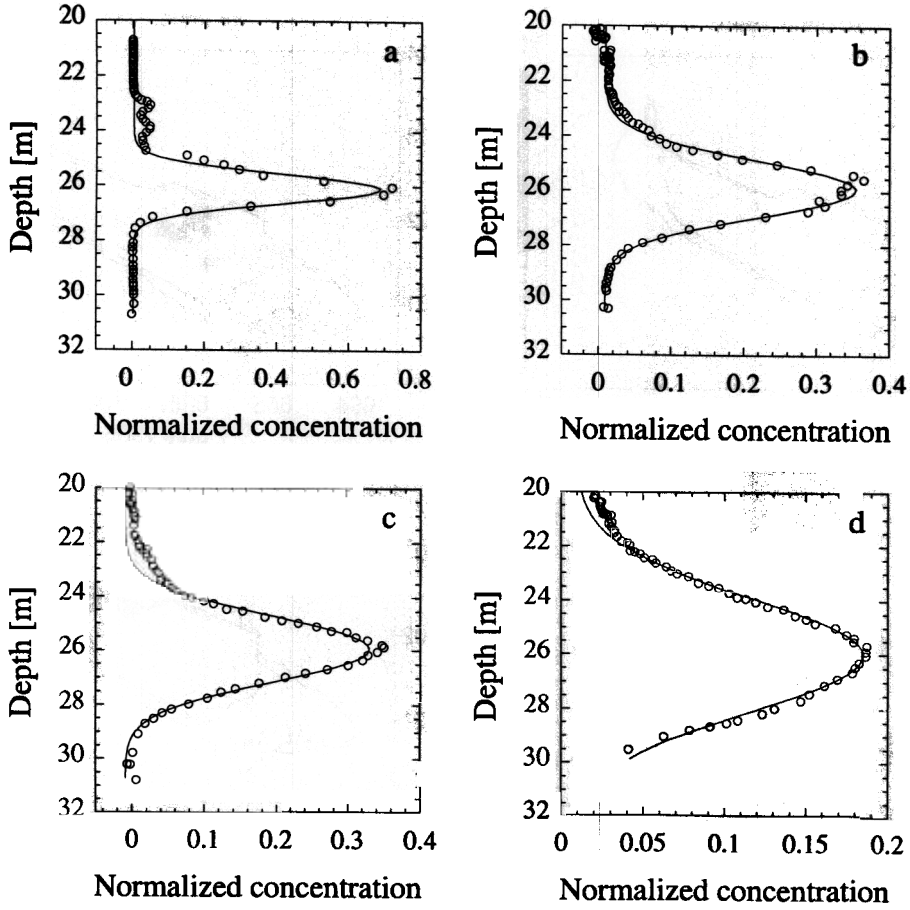

Figure 3. Normalized uranin concentration profiles and curve fits obtained (a) 2, (b) 10, (c) 18, and (d) 25 days after tracer release on June 19, 1995 (experiment III).

As was mentioned before, water density in Lake Alpnach is almost unaffected by dissolved solids (salinity ~ 0.3‰) and hence is determined by temperature. The approximation for density (ρ) of *Bührer and Ambühl* [1975] could therefore be used:

$$\rho(T) = 999.84298\ [\mathrm{kg\ m^{-3}}] + \left(\begin{array}{l} 65.4891\ [\mathrm{kg\ m^{-3}C^{-1}}]T - 8.56272\ [\mathrm{kg\ m^{-3}C^{-2}}]T^2 \\ +0.059385\ [\mathrm{kg\ m^{-3}C^{-3}}]T^3 \end{array}\right) 10^{-3} \quad (1)$$

where T represents temperature in degrees Celsius. Since CTD measurements were carried out only over a limited vertical part of the lake and during a relatively short period, we relied on the temperatures recorded by the moored thermistor strings for the calculation of representative density profiles.

As was mentioned above, local variations in the horizontal tracer distribution can be rather strong, especially in the early stages of such experiments. Although this does not affect the vertical distribution of the averaged tracer profiles, it can affect the absolute concentrations. For example, the fluorometer passed through the center of the tracer cloud more often during some days than during others. Therefore for further examination the mean concentration profiles were normalized, i.e., $\int c_n\, dz = 1$, where c_n represents the normalized uranin concentration. Examples of such normalized profiles are given in Figure 3 (experiment III, 2, 10, 18, and 25 days after tracer release).

3.4. Calculation of K_z From the Tracer Distribution

In the following we assume that the temporal development of the vertical tracer distribution can be described by the one-dimensional diffusion equation

$$\frac{\partial C}{\partial t} = \frac{\partial}{\partial z}\left(K_z \frac{\partial C}{\partial z}\right) = \frac{\partial K_z}{\partial z}\frac{\partial C}{\partial z} + K_z \frac{\partial^2 C}{\partial z^2} \approx K_z \frac{\partial^2 C}{\partial z^2} \quad (2)$$

The so-called pseudo-advection term $(\partial K_z/\partial z)(\partial C/\partial z)$ is negligible in our case because the diffusion coefficient does not vary strongly with depth, as will be shown later. The solution to (2) in a basin with infinite depth assuming an instantaneous, infinitely thin, planar source is

$$C(z,t) = \frac{Q}{2\sqrt{\pi K_z t}} \exp\left(-(z-\bar{z})^2 / 4K_z t\right) \quad (3)$$

where Q denotes the vertically integrated amount of injected tracer (mg m^{-2}), also calculated for experiment III (section 3.1); t is the time since release; and $\bar{z}$ is the mean depth of the tracer cloud. In our case the initial state is, of course, not an infinitely thin plane. However, to a good approximation we can assume that the initial vertical tracer distribution is Gaussian and therefore will remain Gaussian, i.e.,

$$C(z,t) = C(\bar{z},t)\exp\left(-(z-\bar{z})^2 / 2\sigma_z^2(t)\right) \quad (4)$$

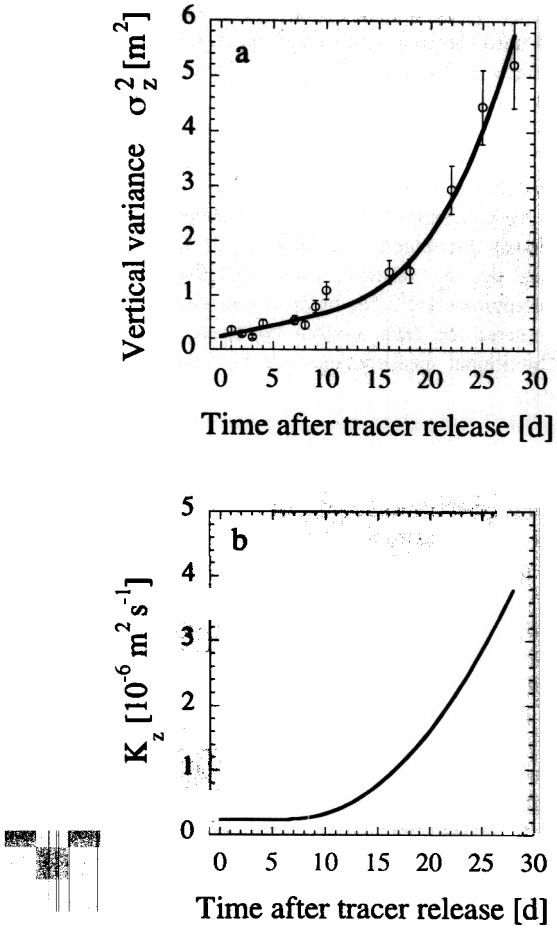

Figure 4. (a) Vertical variances σ_z^2 as a function of time after tracer injection (experiment III, June 19, 1995) with interpolated line. (b) Diapycnal diffusivity K_z computed from equation (5).

Independent of the initial distribution, the vertical variance σ_z^2 is related to the vertical diffusion coefficient K_z by

$$K_z = \frac{1}{2}\frac{\partial \sigma_z^2}{\partial t} \tag{5}$$

In order to determine the vertical variance, all normalized profiles were fitted to Gaussian curves using a least squares algorithm. As an example, normalized and fitted uranin profiles for 2, 10, 18, and 25 days after tracer release in 1995 (experiment III) are shown in Figure 3. The fits clearly agree well with the observed profiles, supporting the assumption of Gaussian profiles. The vertical variances σ_z^2 obtained in experiment III are plotted as a function of time in Figure 4. Vertical eddy diffusion coefficients K_z were obtained by applying (5). In the following sections 4.1-4.3 the numerical results of the analyses will be presented and discussed.

As was mentioned before, (3) is exactly valid only for infinite depth, which is never the case for real basins. However, this restriction is not very critical for experiments I and III. During the first part of the experiment, shortly after tracer release, distances to the lake boundaries are large; later on, when parts of the tracer cloud are close to the bottom boundary, the main part of the tracer cloud is still located in the central water body and not at the boundary. Moreover, horizontal diffusion is much larger than vertical diffusion ($K_x/K_z \approx 10^3$-10^4 [*Imboden and Wüest*, 1995]), and consequently, a local vertical boundary seems not to limit the vertical spreading of a substance rigorously. In experiment II this is certainly not the case (especially not at the beginning of the experiment), as the lake bottom is only a few meters away from the center of mass of the tracer cloud. In addition, vertical mixing is much stronger in the boundary region than in the center of the lake. Thus the lake boundary prevents the tracer from diffusing to greater depth, and the computed vertical variances are therefore smaller than they would be without those boundaries. Consequently, the diffusion coefficients derived from these variances are certainly underestimated. The degree of underestimation is unfortunately unknown because the distance between the center of mass of the tracer cloud and the lake sediment is not constant, varying both with location and time. Immediately after tracer release, for instance, the distance between the sediment-water interface and the tracer is everywhere 2 m, but even after a few hours this is no longer the case. The proper computation of diapycnal diffusion coefficients could only be achieved by applying a true three-dimensional advection-diffusion model. This of course, would go far beyond the scope of our investigation, and therefore we confine ourselves to estimating the diffusion coefficients using (5).

3.5. Calculation of Basin-Wide Diffusivities From Heat Flux Measurements

Independently of the tracer experiments, basin-wide diapycnal eddy diffusion coefficients $\bar{K}_z$ were calculated over the same time and depth intervals as in the tracer experiments by measuring the hypolimnetic heating rate and vertical temperature gradients from quasi-continuously measured temperature profiles at location A (Figure 1). This so-called heat budget method [*Powell and Jassby*, 1974] is based on the assumption that at depth z, the vertical turbulent transport of heat balances the rate of change of the heat content below z. Thus, $\bar{K}_z$ is given by

$$\overline{K_z}(z) = \frac{\int_0^z A(z')\left(\partial T(z')/\partial t\right)dz'}{A(z)\left(\partial T(z)/\partial z\right)} \tag{6}$$

where $A(z)$ is the cross-sectional lake area and $T(z)$ the water temperature at depth z.

To apply this method, temperature oscillations due to seiche motion have to be removed from the temperature record. This was accomplished using linear regression. As was mentioned in the introduction, other heat sources in the hypolimnion can be neglected. According to the meteorological data there were no such events during any of our experiments. For experiment I no thermistor chain data were available, and averaged temperature profiles from CTD casts had to be used instead. However, the estimate for $\partial T/\partial t$ is not as good as those from thermistor chain data, since the influence of internal seiching is not completely filtered out.

In the following section the results of the various experiments are presented. This will not be done in chronological order. The results of the tracer experiments carried out by tracer release in the center of the lake (experiments III and I) are presented first, followed by those of the tracer experiment launched by injection near the boundary layer (experiment II).

4. Results

4.1. Experiment III: Release in the Interior of the Hypolimnion

4.1.1. Diffusivity from uranin data. As was described above, the vertical variances σ_z^2 of the tracer cloud were determined by fitting the normalised uranin concentration profiles to a Gaussian curve. For experiment III the results of this procedure are plotted in Figure 4a. The vertical variance increases slowly at first, but then after about 7 days, it increases much more rapidly. The time of this change coincides with the time when the tracer cloud reached the lake bottom boundary.

In principle, K_z can be computed directly from vertical variances by applying (5). Because of uncertainties in σ_z^2, this would lead to a lot of jitter, and in some cases even to negative diffusivities if the time interval were very short. Therefore, in order to reduce the noise induced by temporal differentiation, a simple empirical function for the time dependence of σ_z^2 was introduced to smooth $\sigma_z^2(t)$.

In a first approach we approximated $\sigma_z^2(t)$ by a linear function

$$\sigma_z^2 = \sigma_z^2(0) + 2K_{z0}t \qquad (7)$$

In the early stages of the experiment (approximately the first 7 days), when the tracer cloud had not yet reached the lake bottom boundary (Plate 1), this approximation is reasonable, as is shown by Figure 4a. Linear regression of the variances over the first 7 days (Figure 4a) yielded a vertical diffusivity of 0.23×10^{-6} m^2s^{-1}. This value can be considered as representative of the vertical rate of mixing in the interior of the hypolimnion (excluding the boundaries).

$K_{z\infty}$ was estimated by analyzing σ_z^2 over the last period of the experiment, i.e., 18-28 days after tracer release. It was assumed that during this period, σ_z^2 increased linearly with time (Figure 4a) and K_z was constant. This approach yielded $K_z = 2.2\times10^{-6}$ m^2s^{-1}, one order of magnitude larger than the initial value. This approach underestimates $K_{z\infty}$ because the tracer cloud is not yet equally distributed horizontally over the entire lake during this period, as can be seen from Plate 1.

Although the linear approximation to σ_z^2 is reasonable, we tried to analyze the data in more detail. As was mentioned above, after the initial period a remarkable increase in vertical spreading can be observed. No analytical relationship for the time dependence of K_z during this period is known because the mixing processes are complex near the local bottom and because of large-scale horizontal advection. The tracer cloud can, for instance, first come into contact with the lake boundaries, then drift away, carried by horizontal currents, then again touch the bottom boundary, and finally undergo horizontally distribution all over the lake area. Prediction of the time dependence of the position and extent of the tracer cloud would thus require a detailed knowledge of the horizontal currents and the vertical diffusion, which would have required an unreasonable amount of effort. We therefore confine ourselves to a semiquantitative description of the entire process.

In a second approach, σ_z^2 for the period after day 7 was smoothed by fitting a third-order polynomial function but taking into account the results of the linear regression from the first 7 days; i.e., σ_z^2, $d\sigma_z^2/dt$, and $d^2\sigma_z^2/dt^2$ should be continuous at t = 7. Figure 4b shows K_z obtained by differentiation of the interpolated curve $\sigma_z^2(t)$. K_z now increases from 0.23×10^{-6} to 3.7×10^{-6} m^2s^{-1}, i.e., by a factor of 16. It must be noted that the value for K_z at the end of the experiment represents a maximum value because it is assumed that the tracer is not equally distributed until the very end of the experiment. Otherwise, K_z would lie between the estimates yielded by the two approaches (linear and polynomial increases in σ_z^2 with time). However, this seems to be a reasonable assumption, as can be seen from Plate 1: only at the very end of the experiment was the tracer more or less homogeneously distributed over the entire lake area. In the following, we will express the diffusivity obtained in the case of homogeneously distributed tracer as $K_{z\infty}$.

Summing up, the vertical diffusivity showed a remarkable increase of approximately one order of magnitude after the tracer had encountered the local bottom boundary. In the following sections, additional measurements are presented to corroborate these results.

4.1.2. Wind measurements. The values obtained for K_z do not represent an average for the whole basin, but only for that volume of the lake in which the tracer has been found. Consequently, the increase in the mixing rate can be explained either by a general increase in diffusion in the entire lake or by the entry of the tracer cloud into a region of higher mixing intensity.

A general increase in the vertical rate of mixing could be induced by stronger wind forcing. This is obviously not the case for the period during which experiment III was carried out, as can be seen in Figure 5. The wind speed shows the already mentioned remarkably regular diurnal pattern due to convection at the adjacent mountains [*Münnich et al.*, 1992]. A general increase in wind speed cannot be observed; on the contrary, there is a slight decline in the mean wind speed after 7 days. Thus the observed sudden increase in vertical mixing cannot be attributed to the onset of stronger wind forcing.

4.1.3. Thermistor chain measurements. The basin-wide vertical diffusivity $\bar{K}_z$ was calculated from (6) over the same time and depth intervals as for the tracer experiment by using the temperature profiles measured by moored thermistor chains. Since the temperature data quality was excellent during experiment III, $\bar{K}_z$ could be determined with the relatively high temporal resolution of approximately 10 days. $\bar{K}_z$ was computed for the same two periods as before: (1) from June 19 to 29 and (2) from July 7 to 17. These intervals were again chosen to distinguish between the periods for which the tracer had not yet encountered the lake bottom boundary (period 1) and had already

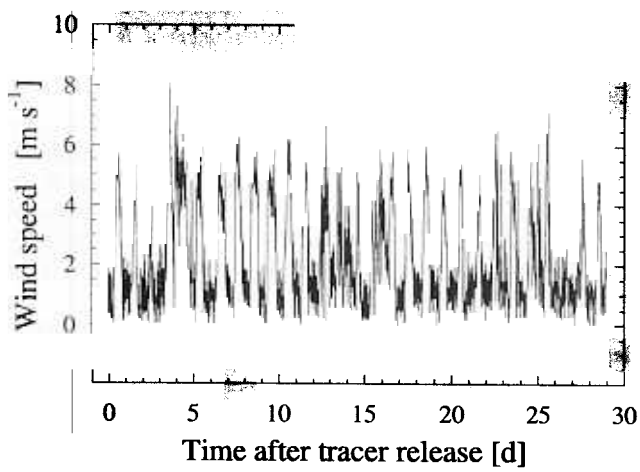

Figure 5. Wind speed at weather station M (Figure 1) for June 19 to July 17, 1995.

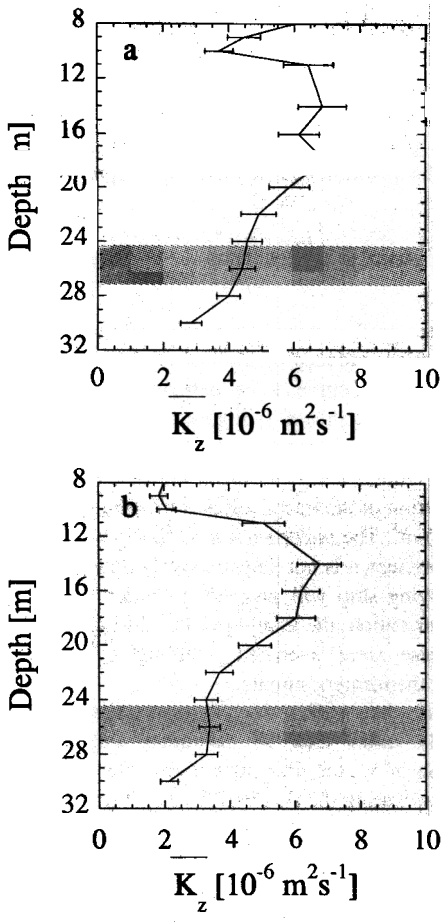

Figure 6. Basin-wide diapycnal diffusivities $\bar{K}_z$ computed using the heat budget method from temperature profiles measured by thermistor chains (experiment III) for (a) June 19-29, 1995 and (b) July 7-17, 1995.

been in contact with it (period 2). The results of the calculations are plotted in Figures 6a and 6b. The diffusion coefficients at the mean tracer depth (~26 m) are somewhat higher for the first period ($\bar{K}_z$ = (4.0±0.5)×10^{-6} m^2s^{-1}) than for the second ($\bar{K}_z$ = (3.5±0.5)×10^{-6} m^2s^{-1}). This decrease in $\bar{K}_z$ seems plausible since the decrease in wind forcing during the experiment implies a decrease in the input of mechanical energy into the lake. The value of $\bar{K}_z$ ((3.5±0.5)×10^{-6} m^2s^{-1}) during the second period (days 18-28) is, within the margin of error, in perfect agreement with the value on July 17 calculated from the tracer experiment.

As the temperature measured by the thermistor chains is homogeneous across the whole lake, the diffusivities calculated from these measurements are basin-wide values. Because of the agreement between both methods at the end of the experiment, the final diapycnal diffusivity obtained from the tracer experiment can be considered to be a representative basin-wide value. This conclusion is supported by the fact that during the last period of the tracer observations, the tracer was spread nearly homogeneously over the entire isopycnal surface, and thus the results obtained from the spreading of the tracer should be representative of the whole basin at the depth of the tracer.

A genuine linear increase in σ_z^2 was not observed because the tracer cloud was not homogeneously distributed until the very end of the experiment. On the one hand, the experiment could not be extended any longer, since near the end of the experiment the tracer signals had declined to a magnitude similar to that of the background (corresponding to ~0.3 mg m^{-3} uranin) and were thus near the limit of detection. On the other hand, the amount of tracer injected could not have been increased, since otherwise the initial tracer concentrations would have been beyond the detection range of the fluorometer (0.01-700 mg m^{-3}). However, in future experiments with long diffusion times, a combination of fluorescent dyes and SF_6 [*Watson et al.*, 1987; *Schlatter et al.*, 1990] for following the initial development of the tracer distribution and the dispersion after horizontal homogeneity, respectively, might solve this problem. A combination of these tracers would seem to be ideal, as it would combine the advantages of both substances: the in situ detection of uranin to explore the initial short-term development, and the high resolution of the SF_6 detection techniques coupled with the high degree of chemical stability of SF_6 to investigate long-term development.

4.2. Experiment I: Release in the Interior

The data of this experiment were analyzed analogously to those of experiment III. Uranin concentrations, measured during various CTD casts, were averaged over individual days by the same procedure already described. Concentration profiles from an individual day were averaged as for experiment III at equal density and then retransformed to the day-averaged depth profile by using the day-averaged vertical density profile. The tracer was

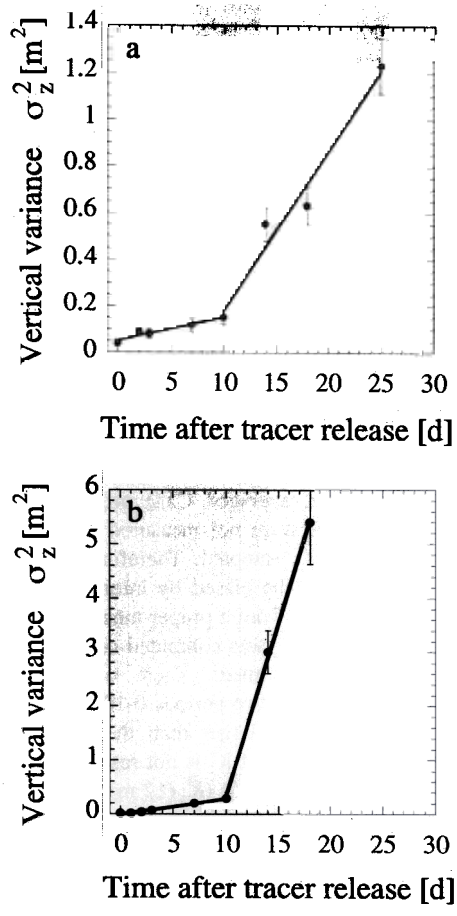

Figure 7. Vertical variances σ_z^2 of the tracer cloud injected on October 12, 1992 (experiment I), at a depth of (a) 22 m and (b) 13 m.

Table 1. Diapycnal Diffusivities Obtained From Tracer Experiments (K_z) and Heat Budget Method ($\bar{K}_z$)

Depth, m	Time After Tracer Release, days	K_z (Uranin), 10^{-6} m^{2}s^{-1}	$\bar{K}_z$ (Temperature), 10^{-6} m^{2}s^{-1}
	October 12 to November 11, 1992 (Experiment I)		
12	0-10	0.17±0.04	4.6±0.5
12	10-25	4±1	
23	0-10	0.06±0.02	0.9±0.4
23	10-25	0.4±0.1	
	June 13-15, 1994 (Experiment II)		
22	0-0.15	80±40	8.5±0.5
22	0.15-2	7±3	
	June 19 to July 17, 1995 (Experiment III)		
25	0-7	0.23±0.04	3.5±1.0
25	7-28	3.7±0.7	

released at 12 m and 23 m depth. The estimated vertical variances and corresponding diapycnal diffusivities (by application of (5)) at both depths are shown in Figure 7.

At both depths a remarkable increase in σ_z^2 was observed 10 days after tracer release. Consequently, again vertical mixing rates increased dramatically from the period 0-10 days to the period 10-25 days after tracer release. Since the amount of data is rather limited, in this case K_z was determined by applying a linear fit to σ_z^2 for each of the two time periods. In 23 m depth, K_z increased from $(0.06\pm0.02)\times10^{-6}$ m^{2}s^{-1} to $(0.4\pm0.1)\times 10^{-6}$ m^{2}s^{-1} (factor of 6) and at 12 m depth from $(0.17\pm0.04)\times10^{-6}$ m^{2}s^{-1} to $(4\pm1)\times10^{-6}$ m^{2}s^{-1} (factor of 25) for 0-10 days and 10-28 days after tracer release, respectively (Table 1). The increase in K_z with time by approximately one order of magnitude is in good agreement with the results of experiment III, again reflecting the effect of boundary mixing.

Since no weather station was installed at the lake shore during the course of the first experiment, data from the nearby official weather stations in Lucerne and Mount Pilatus were used. Both stations show that the daily mean wind speed did not exceed 4 ms^{-1}, thus indicating that no storm could have caused the increase in vertical mixing 10 days after the tracer release.

In order to confirm the value of K_z at the end of the experiment (when the tracer was distributed over the entire lake), $\bar{K}_z$ was again estimated with the heat budget method. Since no thermistor chain data were available, averaged CTD profiles were used. These temperature profiles were not measured as frequently as thermistor data are usually sampled. Therefore even the day-averaged CTD profiles may be biased by internal seiching and may contain some deviations from a proper mean. Consequently, to obtain a robust estimate, $\bar{K}_z$ was computed only for the entire period of time of the experiment. There was no point in subdividing the period into the two periods 0-10 and 10-25 days, as the uncertainties in $\bar{K}_z$ are larger than the differences and therefore the temporal structure of $\bar{K}_z$ is not resolvable. $\bar{K}_z$ at the average depths of both tracer clouds ($\bar{K}_z$ (12 m) = $(4.6\pm0.5)\times10^{-6}$ m^{2}s^{-1} and $\bar{K}_z$ (23 m) = $(0.9\pm0.4)\times10^{-6}$ m^{2}s^{-1}; see Table 1) was, within the margin of error, in good agreement with the results obtained from the tracer experiment.

In this experiment the change in K_z was even more abrupt than in experiment III; i.e., the two diffusion regimes for 0-10 and 10-28 days were even more distinct. It is not clear why this jump should be more pronounced than in experiment III. A possible explanation could be that on the tenth day after tracer release, both tracer clouds drifted to the local bottom boundary and remained there for a significant time period. Under such conditions, diapycnal diffusivity should increase instantaneously, rather than gradually as was observed in experiment III. The data quality is, however, not sufficient either to prove or disprove this hypothesis.

4.3. Experiment II: Tracer Release Near the Sediment-Water Interface

The tracer profiles were again averaged at the same density to avoid distortions induced by internal seiching, and were analyzed by fitting Gaussian curves to the experimental tracer profiles. This yielded the results shown in Figure 8. The initial vertical tracer distribution was estimated from the CTD temperature record shown in Figure 2 and from the effect of initial mixing induced by the injection of the tracer solution into the water to be $\sigma_z^2(t=0) \approx (0.2\pm0.2)$ m^2. The uncertainty in $\sigma_z^2(t=0)$ was estimated on the high side because it is not known exactly how the tracer injection from a moving ship will proceed. In order to verify the initial vertical distribution, the uranin profiles during the first hour after tracer release were averaged, yielding $\sigma_z^2 = 0.5$ m^2, thus confirming the former estimate.

As was expected, the vertical spreading proceeded significantly faster than in the other experiments. For the computation of K_z, the time after tracer release was divided into two periods. During the first period (0 to 7 hours) a major part of the tracer cloud is located close to the region of bottom boundary mixing, and consequently the diffusivity $K_{z1} = (80\pm40)\times10^{-6}$ m^{2}s^{-1} is considerably higher than corresponding values in the other experiments. After this initial period of intense boundary mixing, the tracer cloud spread out horizontally and drifted partially away from the sediment-water interface. Then (7 hours to 2 days) the influence of boundary mixing declined, as the lower value $K_{z2} = (7\pm3)\times10^{-6}$ m^{2}s^{-1} demonstrates.

Again, we tried to compute bulk diapycnal diffusion coefficients from quasi-continuously measured temperature profiles measured by thermistor chains located in the middle of

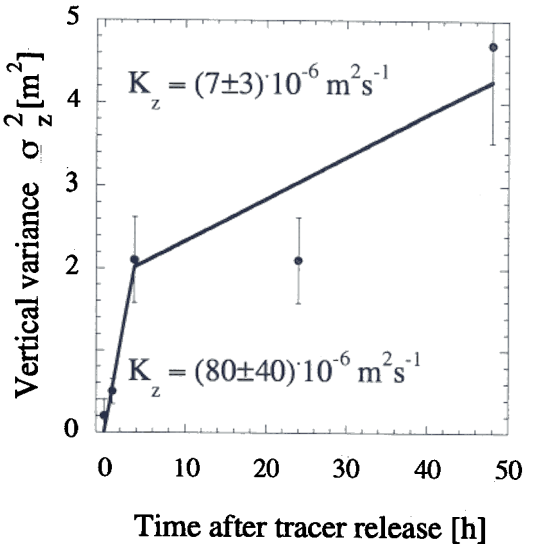

Figure 8. Vertical variances σ_z^2 and diapycnal diffusivities obtained from the experiment conducted in June 1994 (experiment II).

Table 2. Internal, Boundary, and Basin-Wide Diapycnal Diffusivities Obtained From Tracer Experiment, Temperature Profiles, and Temperature Microstructure Profiles

Experiment	Depth, m	Method		
		Tracer (Uranin/SF_6)	Temperature	Microstructure
		Internal K_z, 10^{-6} m^2s^{-1}		
I	12	0.17±0.04		
I	23	0.06±0.02		
III	25	0.23±0.04		
Intercomparison	17	-		0.2±0.08 [a]
		Boundary K_z, 10^{-6} m^2s^{-1}		
II	22	80±40		-
Intercomparison	17			20±10 [b]
		Basin-Wide K_z, 10^{-6} m^2s^{-1}		
	12	4±1	4.6±0.5	
I	23	0.4±0.1	0.9±0.4	
II	22	7±3	8.5±0.5	
III	25	3.7±0.7	3.5±1.0	
Intercomparison	17	3.0±0.4	3.7±0.4	2.5±1.0 [c]

[a] Represents the Gaussian average of $K_z(z)$ relative to 17 m depth (data from *Wüest et al.* [1996]).

[b] This value has been determined by applying the relation $K_z = \gamma_{mix}\, \varepsilon\, N^{-2}$ to the data given by *Wüest et al.* [1996]. Here γ_{mix} is the mixing efficiency (taken as 0.12), and ε and N^2, are the dissipation and the stability within the energetic bottom boundary layer, respectively.

[c] See table of *Wüest et al.* [1996].

the lake near position A (Figure 1). From wind data (not shown), wind excitation during this campaign was more pronounced than during experiment I. Thus we expected to obtain higher bulk mixing rates. The intercomparison of the two methods is limited due to the temporal resolution of the two techniques. In order to remove temperature fluctuations due to internal seiching, we used temperature-time profiles over a period of 10 days. This yielded $\bar{K}_z = (8.5\pm1.0)\times10^{-6}$ m^2s^{-1} for June 8-18, 1994. The tracer experiment, on the other hand, yielded detailed information on mixing processes proceeding on a time scale of less than 2 days (June 13-15, 1994). Moreover, only 2 days after the release, the tracer had not been distributed homogeneously over the entire lake area. Therefore $K_{z2} = (7\pm3)\times10^{-6}$ m^2s^{-1} may contain a larger contribution from boundary mixing than the real value of bulk diapycnal diffusivity after homogenous distribution would have. However, the results of the techniques are in reasonable agreement with one another.

4.4. Comparison With Microstructure Measurements

A study was conducted in July 1989 in Lake Alpnach in order to compare basin-wide diapycnal diffusivities measured by applying tracer techniques (SF_6 and temperature) and microstructure techniques [*Wüest et al.*, 1996]. We confine ourselves here solely to the results of this study (for the technical details, see *Wüest et al.* [1996]). All three approaches yielded the same result within the margin of uncertainty of the methods (Table 2). The microstructure measurements revealed that the turbulence level was indeed remarkably dependent on the location within the water body of the hypolimnion. Consistent with the present study, diffusivity was about 80 times higher (Table 2) within the bottom boundary layer ($K_z = (20\pm10)\times10^{-6}$ m^2s^{-1} (Table 1)), than in the interior of the hypolimnion ($K_z = (0.20\pm0.08)\times 10^{-6}$ m^2s^{-1} (Table 1)). Consequently, it was concluded that basin-wide diapycnal diffusivities lie somewhere in between, averaging the two completely different mixing regimes. Tracer and temperature measurements gave a basin-wide diffusivity of $(3.3\pm0.4)\times10^{-6}$ m^2s^{-1}, quite consistent with the microstructure results (Table 1).

The perfect agreement of the microstructure measurements with experiment III in terms of absolute values for both interior and basin-wide diffusivity may be to some extent accidental. The fact, however, that the turbulence measurements also show the same ratio of interior to basin-wide mixing of ~16 strongly confirms the observations from the tracer study presented here. Therefore, clear conclusions can be drawn that (1) interior mixing is one order of magnitude weaker than basin-wide mixing and that (2) bottom boundary mixing is the dominant process for diapycnal transport in the hypolimnion of medium-sized lakes.

5. Summary

For this work, two types of tracer experiment were conducted in Lake Alpnach. In the first, a tracer solution was injected from a point source in the center of the lake, and its horizontal and vertical spreading was monitored using an in situ fluorometer. During the early stages of this type of experiment, the vertical dispersion of the tracer cloud, and thus vertical diffusivity, was very small, varying from $K_z = (0.6\pm0.2)\times10^{-7}$ m^2s^{-1} at 23 m and $K_z = (1.7\pm0.4)\times10^{-7}$ m^2s^{-1} at 12 m in October 1992 to $K_z = (2.3\pm0.4)\times10^{-7}$ m^2s^{-1} at 25 m in June 1995. After the tracer patches had reached the bottom boundary of the lake, vertical spreading increased dramatically, and corresponding diapycnal diffusivities were approximately one order of magnitude larger than before: $K_z = (0.4\pm0.1)\times10^{-6}$ m^2s^{-1} at 23 m and $K_z = (4\pm1)\times 10^{-6}$ m^2s^{-1} at 12 m in 1992 and $K_z = (3.7\pm0.7)\times10^{-6}$ m^2s^{-1} at 25 m in 1995.

In the second type of experiment, a tracer solution was released near the sediment-water interface. In this case the dynamics of vertical tracer spreading was the reverse: diapycnal diffusivities were large at the beginning of the experiment ($K_z =$

$(80\pm40)\times10^{-6}$ m^2s^{-1} during the first few hours), decreasing markedly (to $\bar{K}_z = (7\pm3)\times10^{-6}$ m^2s^{-1}) after the tracer cloud had partially moved away from the lake boundary.

Both observations can be explained well by a mechanism of enhanced mixing in the bottom boundary region. As soon as, or as long as, a larger part of the tracer cloud is located inside this region, diapycnal diffusion is enhanced, whereas if the tracer patch is situated entirely outside this region, i.e., in the interior of the water column, vertical diffusion is approximately one order of magnitude smaller.

In all experiments, basin-wide diffusion coefficients $\bar{K}_z$ computed independently from heat flux measurements agreed well with those computed from the tracer dispersion after horizontal homogenization of the tracer.

The tracer experiments in Lake Alpnach were conducted during various degrees of seiche activity; accordingly, basin-wide diffusion coefficients $\bar{K}_z$ varied from $(0.9\pm0.4)\times10^{-6}$ m^2s^{-1} to $(8.5\pm0.5)\times10^{-6}$ m^2s^{-1}. Regardless of the conditions under which the study was conducted, the results of the tracer experiments agreed with the conceptual model of boundary mixing. This clearly supports the hypothesis that diapycnal fluxes are predominantly determined by boundary mixing.

The results obtained from the tracer experiments confirm earlier measurements using temperature microstructure techniques, in which estimates of diapycnal diffusivities within the bottom boundary layer also exceeded basin-wide averages by about an order of magnitude, while the basin-wide averages in turn exceeded diffusivities in the interior by an order of magnitude.

Summing up, the results of our tracer investigations give a consistent picture. Diapycnal diffusivity in the hypolimnion of a lake can be described in terms of vertical mixing processes occurring at two different rates: relatively slow mixing in the interior of the lake, and relatively fast mixing within the boundary layers above the sediment-water interface.

Lake size and the magnitude of horizontal transport determine the time required for the tracer to reach the lake boundaries. By choosing, for instance, a large lake or a lake exposed to intense winds, the vertical and horizontal spreading of a tracer can be altered. Future experiments will concentrate on studying the effect of lake geometry and wind excitation on the role of boundary mixing relative to interior water mixing in various different lakes.

Acknowledgments. We are indebted to M. Schurter for his expertise in the field on Lake Alpnach during the entire sampling program, and to V. Matta and D. M. Livingstone for improving the English. This study was supported by Swiss National Science Foundation grants 20-27751.89, 20-32700.91, and 20-36364.92.

References

Armi, L., Some evidence for boundary mixing in the deep ocean, *J. Geophys. Res.*, *83*, 1971-1979, 1978.

Behrens, H., and G. Teichmann, Neue Ergebnisse über den Lichteinfluss auf Fluoreszenztracer, *Beitr. Geol. Schweiz. Hydrol.*, *28*, 69-77, 1982.

Bührer, H., and H. Ambühl, Die Einleitung von gereinigtem Abwasser in Seen, *Schweiz. Z. Hydrol.*, *37*, 347-369, 1975.

Eriksen, C. C., Observations of internal wave reflection off sloping bottoms, *J. Geophys. Res.*, *87*, 525-538, 1982.

Gargett, A. E., Vertical eddy diffusivity in the ocean interior, *J. Mar. Res.*, *42*, 359-393, 1984.

Garrett, C., Marginal mixing theories, *Atmos. Ocean*, *29*, 313-339, 1991.

Gloor, M., Methode der Temperaturmikrostruktur und deren Anwendung auf die Bodengrenzschicht in geschichteten Wasserkörpern, *Diss. ETH, , Nr. 11'336*, p. 159, *Eidgenöss. Tech. Hochschule, Zürich*, 1995.

Gloor, M., A. Wüest, and M. Münnich, Benthic boundary mixing and resuspension induced by internal seiches, *Hydrobiologia*, *284*, 59-68, 1994.

Gregg, M. C., Diapycnal mixing in the thermocline: A review, *J. Geophys. Res.*, *92*, 5249-5286, 1987.

Imboden, D. M., and A. Wüest, Mixing mechanisms in lakes, in *Physics and Chemistry of Lakes*, edited by A. Lerman, D. M. Imboden, and J. R. Gat, pp. 83-138, Springer-Verlag, New-York, 1995.

Ivey, G. N., The role of boundary mixing in the deep ocean, *J. Geophys. Res.*, *92*, 11'873-11'878, 1987.

Ledwell, J. R., and A. Bratkovich, A tracer study of mixing in the Santa Cruz Basin, *J. Geophys. Res.*, *100*, 20'681-20'704, 1995.

Ledwell, J. R., and B. M. Hickey, Evidence for enhanced mixing in the Santa Monica Basin, *J. Geophys. Res.*, *100*, 20'665-20'679, 1995.

Ledwell, J. R., and A. J. Watson, The Santa Monica Basin tracer experiment: A study of diapycnal and isopycnal mixing, *J. Geophys. Res.*, *96*, 8695-8718, 1991.

Ledwell, J. R., A. J. Watson, and C. S. Law, Evidence for slow mixing across the pycnocline from an open-ocean tracer-release experiment, *Nature*, *364*, 701-703, 1993.

Leibundgut, C., Stand und Entwicklung der Tracertechnologie, *Beitr. Geol. Schweiz. Hydrol.*, *28*, 23-35, 1982.

Lueck, R. G., W. R. Crawford, and T. R. Osborn, Turbulence dissipation over the continental slope of Vancouver Island, *J. Phys. Oceanogr.*, *13*, 1809-1818, 1983.

McDougall, T. J., The relative roles of diapycnal and isopycnal mixing on subsurface water mass conversion, *J. Phys. Oceanogr.*, *14*, 1577-1589, 1984.

McDougall, T. J., Thermobaricity, cabbeling, and water-mass conversion, *J. Geophys. Res.*, *92*, 5448-5464, 1987.

Munk, W. H., Abyssal recipes, *Deep Sea Res.*, *13*, 707-730, 1966.

Münnich, M., A. Wüest, and D. M. Imboden, Observations of the second vertical mode of the internal seiche in an alpine lake, *Limnol. Oceanogr.*, *37*, 1705-1719, 1992.

Okubo, A., Oceanic diffusion diagrams, *Deep Sea Res.*, *18*, 789-802, 1971.

Peeters, F., and A. Wüest, Mess-System zur Erfassung dreidimensionaler Tracerverteilung in Seen, *Gas Wasser Abwasser*, *7*, 456-461, 1992.

Peeters, F., A. Wüest, G. Piepke, and D. M. Imboden, Horizontal mixing in lakes, *J. Geophys. Res.*, *101*, 18361-18375, 1996.

Peeters, F., G. Piepke, and M. Gloor, A diffusion model for the development of a boundary layer in lakes, *Aquatic Sciences*, *59*, 95-114, 1997.

Powell, T., and A. Jassby, The estimation of vertical eddy diffusivities below the thermocline in lakes, *Water Resour. Res.*, *10*, 191-198, 1974.

Schlatter, J., M. Hofer, and D. M. Imboden, Die Verwendung von Schwefelhexafluorid zum Studium von Transportprozessen in Seen, *Gas Wasser Abwasser*, *70*, 36-42, 1990.

Smart, P. L., A review of the toxicity of 12 fluorescent dyes used for water tracing, *Beitr. Geol. Schweiz. Hydrol.*, *28*, 101-112, 1982.

Thorpe, S. A., The dynamics of the boundary layers of the deep ocean, *Sci. Prog.*, *72*, 189-206, 1988.

Toole, J. M., K. L. Polzin, and R. W. Schmitt, Estimates of diapycnal mixing in the abyssal ocean, *Science*, *264*, 1120-1123, 1994.

Watson, A. J., M. I. Liddicoat, and J. R. Ledwell, Perfluorodecalin and sulphur hexafluoride as purposeful marine tracers: Some deployement and analysis techniques., *Deep Sea Res.*, *34*, 19-31, 1987.

Wüest, A., D. C. Van Senden, J. Imberger, G. Piepke, and M. Gloor, Comparison of diapycnal diffusivities measured by tracer and microstructure techniques, *Dyn. Atmos. Oceans*, *24*, 27-39, 1996.

M. Gloor, Atmospheric and Oceanic Science Program, Princeton University, Princeton, NJ 08544.

G.-H. Goudsmit, F. Peeters, and A. Wüest, Department of Environmental Physics, Swiss Federal Institute of Environmental Science and Technology (EAWAG) and Swiss Federal Institute of Technology (ETH), Dübendorf, Switzerland. (e-mail: goudsmit@eawag.ch; peeters@eawag.ch; wueest@eawag.ch)

(Received August 6, 1996; revised April 1, 1997; accepted May 7, 1997.)